Stabilization of an earthen material with Tung oil: compaction, strength and hydrophobic enhancement

Citation for published version:
Lin, H, Liu, F, Lourenco, S, Schwantes, G, Trumpf, S, Holohan, D & Beckett, C 2021, 'Stabilization of an earthen material with Tung oil: compaction, strength and hydrophobic enhancement', *Construction and Building Materials*, vol. 290, 123213. https://doi.org/10.1016/j.conbuildmat.2021.123213

Digital Object Identifier (DOI):
10.1016/j.conbuildmat.2021.123213

Link:
Link to publication record in Edinburgh Research Explorer

Document Version:
Peer reviewed version

Published In:
Construction and Building Materials

Stabilization of an earthen material with Tung oil: compaction, strength and hydrophobic enhancement

Lin H.[1#], Liu F.Y.[1], Lourenço S.D.N.[1]*, Schwantes G.[2], Trumpf S.[3], Holohan D.[4], Beckett C.[5]

[1] Department of Civil Engineering, The University of Hong Kong, Pokfulam Road, Hong Kong SAR

[2] Institute for Cultural Heritage Conservation, Shanghai University, Baoshan Campus, Shanghai, PR China

[3] Division of Landscape Architecture, Faculty of Architecture, The University of Hong Kong, Pokfulam Road, Hong Kong SAR

[4] Department of Architecture, Faculty of Architecture, The University of Hong Kong, Pokfulam Road, Hong Kong SAR

[5] School of Engineering, The University of Edinburgh, King's Buildings, Edinburgh

** Corresponding author*

 # Currently at Department of Civil Engineering, Sun Yat-Sen University, Zhuhai, PR China

Abstract

Earthen construction generates interest due to its environmental and economic advantages such as low embodied energy, thermal comfort and low construction cost. Two challenges, namely durability and strength, hinder its application. Tung oil, a sustainable vegetable oil traditionally applied in waterproofing wooden construction, could improve the water resistance and strength of earthen materials. This study aims to detail the multiple roles and mechanisms of Tung oil as a stabilizer. Completely decomposed granite, a natural mineral soil, was selected to assess the influence of Tung oil and its time-hardening behavior on the compaction behaviour, unconfined compressive strength and hydrophobicity. Results revealed that: (1) fresh Tung oil could simultaneously increase the density of compacted soils and decrease the water required for compaction. (2) Tung oil hardened during drying, bonding soil particles and enhancing the unconfined compressive strength of the compacted soils. (3) Hydrophobicity of the stabilized soils were also enhanced, with high and persistent contact angles, which could further contribute to its durability and minimize water-induced damage.

Key words: earthen materials; stabilizers; Tung oil; hydrophobicity; compaction; strength

Introduction

Earthen materials have been used as building elements in walls, shelters and floors for thousands of years (Easton, 2007; Walker *et al.,* 2005). Compared to traditional civil engineering materials, they have significant environmental benefits including low embodied energy and carbon footprint (Treloar *et al.*, 2001; Hall and Allinson, 2009; Arrigoni *et al.*, 2017). However, two key limitations remain, mostly related to their low strength and durability.

Unstabilized earthen materials (*i.e.,* without any cementing or bonding additives) have a relatively low strength, comparing to other traditional construction materials such as concrete and steel. For example, Lin *et al.* (2017) tested rammed earth formed from three representative soils in Hong Kong (residual soil, alluvium and completely decomposed granite), revealing their compressive strength to be generally lower than 2.0 MPa. Comparable results have also been reported from other soils in different regions *e.g.,* 1.9-2.5 MPa in Aguilar *et al.* (2016) and 1.7 MPa in Luo *et al.* (2020). As a soil-based material, its mechanical behavior is also affected by the soil water content. The role of suction (or capillary pressure) of unsaturated soils is now recognized as a key factor controlling their strength and stability (Jaquin *et al.*, 2009). In humid areas, for instance, rammed earth has a decreased strength (Beckett *et al.*, 2018; Bui *et al.,* 2014; Jaquin *et al.,* 2009) due to the higher water content and low suction. Inadequate durability related to the presence and action of water is another concern. Erosion and desiccation cracks of earthen buildings can be triggered by rainfall, wind and wetting-drying cycles (Bui *et al.,* 2009). For example, recently Luo *et al.* (2020) reported erosion, due to wind-driven rain, and desiccation cracks, due to drying, on the earthen walls of the UNESCO World Heritage site of Tulou (Fujian Province, China).

To address these two key challenges, efforts have been made to use hydrophobic coatings to prevent erosion and stabilizers to improve strength. For example, Nakamatsu *et al.* (2017) used carrageenan to ameliorate the durability of earthen construction. Silane-based materials have also been used as hydrophobic coatings and have proven effective in monuments and historical earthen buildings with no ill effect on their strength (*e.g.* Holub *et al.*, 2015). Using cementing or bonding additives in the soil matrix (or so-called stabilizers or integral admixtures) to enhance the strength is widely accepted. The most long-established stabilizers are cement and lime which have been used for hundreds of years (Easton, 2007). These stabilizers increase the compressive strength of rammed earth to 10~20 MPa (Ciancio and Gibbings, 2012; Gu and Chen, 2020; Reddy *et al.,* 2008; Reddy and Kumar, 2011). However, they have high carbon footprint and embodied energies. Maskell *et al.* (2014) reported that using more than approximately 10% of cement or lime as stabilizers can offset the embodied energy advantage of the earthen construction.

In order to resolve the strength and durability challenges simultaneously, hydrophobic stabilizers have been proposed which can not only improve the water resistance by inducing soil hydrophobicity (*i.e.,* the matrix is hydrophobic), but also enhance the mechanical properties. For example, Zhang *et al.* (2020) explored the use of polyvinyl acetate (PVA) as a hydrophobic stabilizer to induce soil hydrophobicity and protect earthen construction from erosion. Aguilar *et al.* (2016) reported that chitosan increases the strength of rammed earth and generates soil hydrophobicity simultaneously. Fatty acids such as stearates and oleates combined with cement are also able to achieve a hydrophobic effect for earthen buildings (Eires *et al*., 2017; Nagaraj and Muguda, 2020).

Among these hydrophobic stabilizers, Tung oil is a promising substance given its natural origin, cost-effectiveness and its ability to improve both the mechanical behavior and water resistance in soils (Samadzadeh *et al.*, 2011; Yang *et al.*, 2015; Li *et al.*, 2018). Tung oil is a traditional Chinese vegetable oil abstracted from the Tung tree (*Vernicia fordii*). As a drying oil with a high content of unsaturated fatty acids, Tung oil can be hardened when exposed to the atmosphere (Schönemann and Edwards, 2011). Its most common use is for wood preservatives, where it is applied solely, or in combination with lime, water and flour as part of an elaborate multi-layered process (Fu *et al.,* 2020). Moreover, Tung oil has had other uses historically, including as an organic additive to enhance specific properties of lime mortars, as a primary constituent of caulking applied directly between the wooden boards of ships, and as a protective waterproofing layer in masonry construction (Xing *et al.,* 1995). Recently, Tung oil has been extended to other construction materials such as self-healing concrete and asphalt (Chen *et al.,* 2017; Fang *et al.,* 2014; Qiang *et al.,* 2014; Xin *et al.,* 2016; Yan *et al.,* 2020).

Of interest to earthen materials, Dai (2013) investigated the traditional technique of adding Tung oil and lime to rammed earth to enhance the water resistance and tested different concentrations of raw Tung oil in the mixture of clay soil and calcium hydrate (10 %), with results showing that 5% Tung oil is the optimum dosage to reduce the capillary water uptake of the rammed earth. However, lime alone also has a stabilizing effect on clayey soils and their study does not differentiate whether the improved properties are a result of either or both additives. Zhang *et al.* (2016) considered the use of Tung oil to enhance the water resistance of earthen monuments. Tang *et al.* (2010) mixed the soils with Tung oil and sticky rice juice to ameliorate its durability under wetting-drying cycles, and explored its use to reduce water infiltration in a clayey soil (Tang *et al.*, 2006). Lin *et al.* (2019) investigated the effects of Tung oil (heated and unheated) on soil hydrophobicity and the strength of soil aggregates, showing that by using high temperature, soil can be more hydrophobic and consequently the consumption of Tung oil can be saved. At the same time, water stability and tensile strength of soil aggregates are also enhanced by Tung oil and heating. From these observations, Tung oil shows potential in earthen materials as a hydrophobic stabilizer. However, the published studies do not investigate the improvement of the soil properties, *i.e.* mechanics and hydrophobicity, with Tung oil concentration and time to account for the hardening effect, and its implications for earthen construction remains unresolved.

This study aims to detail the multiple roles of Tung oil in improving properties of earthen materials with time. The specific objectives are (1) to investigate the effect of Tung oil concentration and its time-dependent hardening behaviour on soil compaction, compressive strength and hydrophobicity and, (2) to elucidate the controlling mechanisms of the stabilization of Tung oil in soils. Three sets of tests corresponding to these properties were carried out, namely modified compaction tests, unconfined compressive tests and soil hydrophobicity assessment (Fig. 1).

Materials

Completely decomposed granite

Completely decomposed granite (CDG) used in this study was collected from Beacon Hill, Hong Kong. CDG is a mineral soil prevalent in Hong Kong where the sub-tropical climate has weathered its parent rocks (granite) to a material comprising sand, silt and clay-sized particles. To determine the particle size, CDG was firstly wet sieved through a 63-μm mesh. The coarse fraction (*i.e.,* soils retained on the mesh) was oven dried and analysed by a dynamic image analyser, QicPic™ (Sympatec GmbH, Clausthal-Zellerfeld, Germany) through a gravity dispenser (GRADIS™), while the fines dispersed in water were analysed by QicPic™ through a wet dispersion unit (LIXELL™). The particle size distribution of CDG is shown in Fig. 2 and complies with general guidance on suitable gradings for earthen construction (*e.g.,* Walker *et al.,* 2005). Mineralogical composition of CDG comprises quartz, microcline, kaolinite and illite as detected by X-ray diffraction (XRD). CDG contained limited organic matter (<2%) which was determined by loss on ignition test (LOI, following BS 1377-3:1990). Soil specimens were firstly air dried at ambient temperature (20~25°C) for three days so that the soil water content was lower than 3%. Soil properties are summarized in Table 1.

Tung oil

The Tung oil used in this study is a commercial product from Jogel Co., China. It contained approximately 80% of alpha-eleostearic acid, and 20% of other fatty acids (linoleic, oleic and palmitic acid) which are known to induce soil hydrophobicity (Lin *et al.,* 2019; Schönemann and Edwards, 2011) and was used in a raw state, *i.e.* without further additives. The properties of Tung oil are listed in Table 2.

Experimental program

Modified compaction test

Geotechnical materials are frequently compacted in samples with a volume 1000 cm^3 when examining compacted dry densities. To allow the testing of a greater number of samples, Sridharan and Sivapullaiah (2005) proposed a modified compaction test (MCT) with smaller mould dimensions. Here, to accelerate the equilibration process of specimens (both water content and Tung oil hardening), the MCT test was adopted with a mould volume of 85.06 cm^3 (36.5 mm diameter by 105 mm height) which was more than 10 times larger than the largest particle size of CDG, a requirement set by Sridharan and Sivapullaiah (2005).

It is well understood that the dry density influences the mechanical properties of earthen materials and that multiple pore network architectures can exist for a given dry density, depending on the strength of the soil aggregates. To isolate the effect of Tung oil, the energy per unit volume (e_c), rather than dry density, was controlled and kept similar to the Standard Proctor Test (SPT) following Eq. (1).

$$e_c = E_{SPT}/V_{SPT} = \left(n_{SPT} \times l_{SPT} \times m_{SPT} \times g \times h_{SPT}\right)/V_{SPT} \qquad \text{(Eq. 1)}$$

Where E_{SPT} is the total input energy, V_{SPT} is the volume of the mould, n_{SPT} is the number of blows per layer, l_{SPT} is the number of layers, m is the mass of the rammer, g is the gravity acceleration and h_{SPT} is the falling height per blow. The subscript *SPT* refers to Standard Proctor Test. By reducing the number of blows from 25 (SPT) to 17 (MCT), e_c in the MCT was kept similar to the SPT (Ciancio *et al.*, 2013): 572 J and 594 J, respectively. Testing parameters used in the MCT are listed in Table 3, in which the parameters of the SPT are also attached as a reference.

Tung oil is able to harden after mixing with soils within 7 days due to oxidative polymerization (Lin and Lourenço, 2020; Tang *et al.*, 2010; Tang *et al.*, 2006). To investigate this hardening effect on the compaction behaviour, MCT tests were conducted immediately after mixing with Tung oil (hereinafter *fresh stabilized soils*) and after 7-day equilibrium (*hardened stabilized soils*). Testing procedures are detailed next.

For the fresh stabilized soils, a given concentration of Tung oil (0, 1, 5, 8, 10 and 15%) was firstly mixed with 1.0 kg of CDG. This concentration range was based on preliminary tests and other works (*e.g.,* Lin *et al.,* 2019; Tang *et al.,* 2006) where 5~10% of Tung oil can induce extreme soil hydrophobicity. After that, water was immediately added to the mixed soils (10~28%) and compaction was conducted. For the hardened stabilized soils, Tung oil was mixed with 1.0 kg of CDG and then equilibrated at an ambient condition for 7-days (20~25°C, relative humidity = 70~85%). Then, the stabilized soils were wetted to the same water content range and compacted.

Unconfined compression test

CDG specimens with two Tung oil concentrations (5 and 10%) were selected for unconfined compression test based on the results of the modified compaction test, where lower and higher concentrations were discarded because 1% of Tung oil had a minor effect on compaction and 15% made CDG too hydrophobic to be wetted. The CDG specimens with 0% (*i.e.* control), 5% and 10% of fresh Tung oil were firstly wetted to achieve the optimum moisture content of the stabilized soils with respective concentrations of Tung oil, and then compacted in a cylindrical mould with dimensions 36.5 mm diameter by 105 mm height, as described in Section 3.1. After compaction, these specimens were equilibrated at ambient temperature (20~25°C) for 3, 7 and 28 days. Specimens were tested in a universal compression machine (Tritech 50, Wykeham Farrance, United Kingdom) in strain-controlled conditions with the displacement rate of 1.0 mm/min (BS 1924-2:2018).

Hydrophobicity measurement

Hydrophobicity of granular materials can be quantified by two widely-used parameters, namely water drop penetration time (WDPT) and contact angle (CA) (Leelamanie *et al.,* 2008; Wessel, 1988). All CA and WDPT tests were conducted in disturbed (uncompacted) stabilized soils which had a lower density. This led to a more conservative measurement of hydrophobicity because soil specimens with larger void size had a lower contact angle and shorter WDPT. The WDPT test was originally developed in soil science and involves placing a water drop on a surface of particles and recording the time taken for its full penetration (Letey *et al.,* 2000); the time therefore reflects the treatment's persistency.

CA reflects the severicity of soil hydrophobicity. CA is obtained from Young's equation (Eq. 2). The equation is derived from the mechanical equilibrium of a water drop on a flat surface with three interfacial tensions, solid-liquid γ_{sl}, solid-air γ_{sa} and liquid-air γ_{la}.

$$cos\theta = \frac{\gamma_{sa}-\gamma_{sl}}{\gamma_{la}} \quad \text{(Eq. 2)}$$

Higher CA shows the earthen material has greater hydrophobicity, and subsequently a higher water resistance.

In this study, hydrophobicity was measured after 3, 7 and 28 days of equilibrium, the same times as used for the uniaxial compressive strength test. WDPT test was carried out by placing a 50μL of water drop on a stamped granular surface. The penetration time was recorded with an upper limit of 3600s. CA was measured by sessile drop method (SDM) proposed by Bachmann *et al.* (2000) with a Drop Shape Analyser (KRÜSS GmbH, Hamburg, Germany). A schematic of SDM is shown in Fig. 3. Stabilized soils were firstly sprayed on a double-sided tape on a glass slide. A 10μL of water drop was placed on the soil surface. Its shape was recorded by a camera and CAs was determined by a curve-fitting algorithm (Saulick *et al.,* 2018). Note that the CAs measured in soils, including the ones reported in this paper, are apparent CAs to account for the roughness and porous nature of the soil together with the surface chemistry. Intrinsic CAs only account for the molecular composition of a surface and its interaction with liquid water.

FTIR spectra and SEM imaging

To elucidate the mechanisms controlling the hardening of Tung oil stabilized soils, FTIR analyses were conducted in fresh and hardened stabilized soils using a FTIR spectrometer: a PerkinElmer

Spectrum 100 with an accuracy of 1 cm^{-1}. Soil specimens were prepared by the KBr pellet method. The particle surface and microstructure of stabilized soils were investigated with scanning electron microscope (SEM, Leo 1530 FEG).

Results

Compaction behaviour

For fresh stabilized soils (*i.e.,* soils stabilized with Tung oil in a fresh liquid state), a higher concentration of Tung oil reduced the optimum moisture content (OMC) while increasing the maximum dry density (MDD), as illustrated in Fig. 4. For example, the OMC of natural CDG was 23% and corresponding MDD was 1.59 g/cm^3. With 5% of Tung oil, the OMC reduced to 17% and MDD increased to 1.65 g/cm^3. OMC continuously decreased and MDD rose at greater concentrations. Obtained MDDs were lower than might be considered for rammed earth construction but are comparable to construction typologies receiving less compaction, for example shuttered cob (Walker *et al.,* 2005).

The compaction behaviour differed for the hardened stabilized soils. Fig. 4b shows the compaction curves of stabilized soils after equilibrating for 7-days. In this case, the OMC decreased with Tung oil concentration but MDD remained unchanged. For instance, comparing to natural CDG (OMC=23% and MDD=1.59 g/cm^3), soils with 10% of hardened Tung oil had lower OMC (13%) but MDD was almost equivalent (1.60 g/cm^3).

A comparison of OMC and MDD between fresh and hardened stabilized soils is plotted in Fig. 5. In both cases, Tung oil decreased the OMC during the compaction (Fig. 5a). The effect on OMC was comparable between fresh and hardened specimens. As for MDD, in fresh stabilized soils, the value increased with Tung oil concentration, but in the hardened samples, compaction did not yield higher MDD at higher concentrations. For example, MDD of 1% Tung oil was 1.6 g/cm^3 in fresh samples and continuously increased to 1.68 g/cm^3 at 10%, while the corresponding MDD of the hardened sample was comparable at 1% (1.59 g/cm^3) but remained unchanged at 10%.

Unconfined compression strength

The UCS of stabilized soils increased with the concentration of Tung oil and hardening time. Fig. 6 illustrates the increase of UCS of natural and stabilized soils. Without Tung oil, natural CDG soil (control sample) had a slight increase in compression strength from 632 kPa on the 3rd day to 687 kPa on the 28th day; 5% of Tung oil resulted in a higher strength, from 1853 kPa at 3 days to 2136 kPa after the 28-day equilibration. A higher concentration (10%) further enhanced UCS to 2217kPa at 3 days and 2641 kPa after 28 days.

Hydrophobicity

Soil hydrophobicity, quantified by CA and WDPT, increased with Tung oil concentration and time in stabilized soils. Fig. 7 shows the increase of CA and WDPT with Tung oil concentration during 28-day hardening. The initial CA of natural CDG ranged from 70.3 to 71.8°. Tung oil concentration induced higher CAs from 94.6° at 1% to 110.5° at 15%. The CAs continued to increase up to day 7, becoming stable on the 28th day. For example, the CA of specimens with 5% of Tung oil ranged from 101.6° on day 0, to 115.7° and 117.9° after 7 and 28 days, respectively. WDPT showed the same tendency, *i.e.* increasing persistency with time and Tung oil concentration.

FTIR spectra and SEM imaging

Mineral composition and chemical changes due to the presence of Tung oil were reflected by the FTIR spectrum of natural and stabilized CDG as shown in Fig. 8. Absorption in the region of 3750-3570 cm^{-1} represented the hydroxyl (O-H) stretching vibrations of kaolinite in CDG (Mckissock *et al.*, 2013). The bands at 1101 cm^{-1}, 1033 cm^{-1} and 913 cm^{-1} are from in-plane Si-O stretching, out-of-plane symmetric Si-O stretching, and O-H deformation of kaolinite, respectively (Linker *et al.*, 2005). The absorption of 797 cm^{-1} can be identified in the spectrum, which is the fingerprint region of quartz (from CDG). Hematite is identified by the peak at 539 cm^{-1} (Salama *et al.*, 2015). The spectrum of fresh stabilized CDG had three identifiable peaks at 2926, 2856 and 1746 cm^{-1}. Given the existence of hydroxyl (O-H) in kaolinite (3750-3570cm^{-1}), O-H stretching vibrations from Tung oil could not be differentiated. Typical C-H stretching of aliphatic -CH=CH- is at around 3010cm^{-1} (Grehk *et al.*, 2008), but this was not detected in Fig. 8. A possible reason is the limited concentration of Tung oil in the stabilized soil. The peaks at 2926 cm^{-1} and 2856 cm^{-1} are the symmetric and asymmetric C-H stretching vibration of the methyl group (Schönemann and Edwards, 2011). These methyl groups were mostly from alpha-eleostearic acids (representing ~80% of the Tung oil). The peak at 1746 cm^{-1} was attributed to hydrogen-bonded carboxyl groups. The 7-day equilibrium resulted in the oxidative polymerization of Tung oil, which was reflected by the shifts of 2926 and 2856 cm^{-1} peaks to 2931 and 2858 cm^{-1} (Schönemann and Edwards, 2011; Lin *et al.*, 2019). At the same time, a generated peak at 1637 cm^{-1} suggested COO- groups formed during the equilibrium.

SEM images (Fig. 9) show the natural (untreated) soil particles and particles covered with hardened Tung oil. In natural CDG, silica sand particles were covered by fines comprising kaolinite and illite based on the XRD results (Section 2.1). Clay minerals are hydrophilic (Mgbemena *et al.,* 2013; Lourenço *et al.,* 2015) and consequently CDG has a low contact angle

(~70°). Imaging of stabilized CDG reveals a Tung oil coating covering the whole surface of the particles (Fig. 9b). These are either (1) large quartz particles covered with fines (mostly kaolinite) and Tung oil or (2) several quartz particles with fines bonded and covered by Tung oil. Tung oil has been reported to bond particles (*i.e.,* aggregation) (Lin *et al.,* 2019). Tung oil films are slightly hydrophobic with CA ranging from 90° to 95° (*e.g.,* Arminger *et al.*, 2020). When coated onto the soil particles, the CA measured can be higher due to the rough surface of the particles (Saulick *et al.*, 2018; Saulick *et al.*, 2020).

Discussion

Mechanisms

Tung oil was found to enhance compaction, compressive strength and hydrophobicity. The controlling mechanisms for compaction and compressive strength are three-fold and may be attributed to changes in suction, inter-particle friction and bonding (analogous to cohesion or cementation) (Fig. 11). For compaction enhancement (Fig. 4 and Fig. 5), a combination of suction and inter-particle friction is likely to dominate. As the particles' surfaces are now hydrophobic, suction is lower (for a given amount of water), increasing the deformability of the soil aggregates and allowing grains to be arranged in closer packings. The fresh Tung oil coatings in a liquid state may also change the inter-particle friction as the inter-particle contacts are no longer mineral to mineral. Although such mechanisms have yet to be examined for Tung oil, Lourenço *et al.* (2018) showed that polydimethylsiloxane (PDMS) coatings smooth the soil particle surfaces. Liu *et al.* (2019a, 2019b) investigated the mechanical behaviour of PDMS-coated sands through triaxial tests and inter-particle friction tests, revealing that coatings can alter the dilatancy, critical state and inter-particle friction. However, in hardened stabilized soils, higher concentrations of Tung oil did not increase the dry density. A possible reason is that adding Tung oil resulted in the aggregation of soil particles which could strengthen during the 7-day equilibrium. During compaction, these hardened aggregates had to be firstly crushed, followed by the re-arrangement of soil particles, resulting in looser soil packings and a lower dry density.

As for the compressive strength enhancement, soil aggregation was observed in the hardened stabilized soils. Lin *et al.* (2019) tested the compressive strength of the fresh soil aggregates and aggregates after heating (where Tung oil underwent oxidative polymerization and hardened during heating), revealing that the tensile strength of fresh aggregates were negligible while for hardened aggregates the tensile strength was 200~800 kPa, depending on the Tung oil concentration and heating conditions. Therefore, the strength enhancement during the equilibrium (Fig. 6) is assumed to be related to the solidification of Tung oil bonding the soil particles.

The hydrophobic enhancement (Fig. 7) correlates with the Tung oil concentration and time. The increasing CA and WDPT at time 0 may be related to increasing aggregate size with Tung oil concentration (Lin *et al.*, 2019) and the filling of intra-aggregate pores with Tung oil. As for the time-dependent increase, this phenomenon may be related to the oxidative polymerization of Tung oil which gradually switches the liquid coating into a solid phase (Arminger *et al.*, 2020). The Tung oil reaction consists on the oxidation and polymerization of unsaturated fatty acids, which decrease the viscosity of Tung oil and form solid or semi-solid films (Grehk *et al.*, 2008; Arminger *et al.*, 2020; Fuller, 1931). This process requires the double bonds in unsaturated fatty acids to react with oxygen from the air, forming a crosslinked network (Fig. 10). Note that while this process explains the hardening of Tung oil, it does not explain the hydrophobic enhancement. In allied fields, the drying and hardening of thin oil films (for paintings, for instance) has been studied but its relation to hydrophobicity has not been established (*e.g.*, Lazzari and Chiantori, 1999). Further research is needed to identify the mechanisms controlling hydrophobic enhancement in hardening Tung oil films.

Implications for earthen construction

Nowadays construction of earthen buildings is focusing more and more on detailed investigation of traditional practices as well as reviving traditional craftsmanship as a basis of informed decision making for sustainable construction. Dealing with follow up damage of past earthen structures, engineers concluded that chemical and physical compatibility are the most important quality of a successful construction. Traditional techniques are investigated scientifically to understand the chemical and microstructural processes and utilize this deeper understanding to create the building materials with similar or improved properties.

From the outcomes of this study, the difference of compaction behaviour between fresh and hardened stabilized soils indicates that in order to achieve a high density, the compaction time (*i.e.,* the time between mixing and compaction) should be shorter than the hardening time of Tung oil (7 days). The hardening time depends on the type of Tung oil, temperature and sunlight ranging from a few hours to one day (Arminger *et al.,* 2020; Fang *et al.,* 2014). Water savings during compaction can also be accrued, as the optimum moisture content of Tung oil-stabilized soils is relatively lower than the untreated one.

The compressive strength of compacted stabilized soils can be increased to more than 2.6 MPa within 7 days suggesting the suitability of Tung oil as a stabilizer. This strength enhancement is lower than cement (~15 MPa) but comparable to novel stabilizers such as calcium carbide residue combined with fly ash (~2.5 MPa, Siddiqua and Barreto, 2018), Carrageenan (~3.8 MPa, Nakamatsu *et al.*, 2017b), and chitosan (~3.8 MPa, Aguilar *et al.,* 2016). For compacted soils, the lower bound of unconfined compressive strength is variable in the literature. For example, NZS 4298 (2020) standard proposes that the strength should be larger than 1.1 MPa (for 2:1 compacted cylindrical specimens) while Walker *et al.* (2005) suggested 1.0 MPa as adequate. Ciancio *et al.* (2013) suggested 0.2 MPa was sufficient for non-load bearing walls (although this low strength has repercussions for durability). As for the hardening period, the results show that 85% of the ultimate UCS can develop within 7-days. Comparing to other stabilizers, Tung oil has a faster strength development. For example, the calcium carbide residue-fly ash stabilizer required at least 28 days to achieve 80% of ultimate UCS (Siddiqua and Barreto, 2018), and this hardening time is comparable to cement-stabilized rammed earth (Arrigoni *et al.,* 2017; Hall and Allinson, 2009; Reddy *et al.,* 2008).

Tung oil can induce high and persistent hydrophobicity in CDG, as demonstrated by CA ~117° and WDPT >3600 seconds (Fig. 7). The fact that the earthen matrix shows hydrophobic properties, represents an added advantage as it might delay its decay from weathering and erosion and prolong its longevity (Meek *et al.*, 2020).

Conclusions

The effect of Tung oil and its time-dependent hardening behaviour on the mechanical and hydrophobic behavior of a compacted soil has been investigated. Different concentrations of Tung oil were added and mixed with completely decomposed granite, a widespread mineral soil from Hong Kong. Modified compaction tests, unconfined compression strength and hydrophobicity measurements (contact angles and water drop penetration time) were performed and the analysis of the results were supported by elemental characterization and surface imaging. Major outcomes are as follows:

1. Mixing the soil with fresh (liquid) Tung oil creates an aggregated soil structure which hardens with time;
2. Compacting the soil with fresh (liquid) Tung oil results in a higher dry density and lower optimum moisture content, while for soils with hardened Tung oil the dry density had no relation with Tung oil concentration;
3. The compressive strength of the stabilized soil increased with Tung oil concentration and hardening time;
4. Soil hydrophobicity was imparted by Tung oil and enhanced with hardening time.

These results showed that Tung oil is a promising stabilizer for earthen materials because of its benefits on (1) increasing the dry density, (2) increasing the compression strength and (3) inducing soil hydrophobicity which may further improve its durability. The results and analysis presented in this study provide a record for reviving a traditional technique and a basis for utilizing it to construction of earthen buildings, as well as conservation and interventions for earthen architecture heritage sites. Future work should focus on the durability, environmental impact and life-cycle assessment of Tung oil-stabilized earthen construction.

Acknowledgements

This work was supported by the General Research Fund (Grant 106170078) from the Research Grants Council of Hong Kong Special Administrative Region, China

References

Aguilar, R., Nakamatsu, J., Ramírez, E., Elgegren, M., Ayarza, J., Kim, S., Pando, M. A., & Ortega-San-Martin, L. (2016). The potential use of chitosan as a biopolymer additive for enhanced mechanical properties and water resistance of earthen construction. *Construction and Building Materials*, *114*, 625–637. https://doi.org/10.1016/j.conbuildmat.2016.03.218

Arminger, B., Jaxel, J., Bacher, M., Gindl-Altmutter, W., & Hansmann, C. (2020). On the drying behavior of natural oils used for solid wood finishing. *Progress in Organic Coatings*, *148*(April), 105831. https://doi.org/10.1016/j.porgcoat.2020.105831

Arrigoni, A., Pelosato, R., Dotelli, G., Beckett, C. T. S., & Ciancio, D. (2017). Weathering's beneficial effect on waste-stabilised rammed earth: a chemical and microstructural investigation. *Construction and Building Materials*, *140*, 157–166. https://doi.org/10.1016/j.conbuildmat.2017.02.009

Bachmann, J., Horton, R., Van Der Ploeg, R. R., & Woche, S. (2000). Modified sessile drop method for assessing initial soil–water contact angle of sandy soil. *Soil Science Society of America Journal*, *64*(2), 564–567.

Beckett, C., & Augarde, C. (2012). The Effect of Relative Humidity and Temperature on the Unconfined Compressive Strength of Rammed Earth. *Unsaturated Soils: Research and Applications*, 287–292. https://doi.org/10.1007/978-3-642-31116-1_39

Bui, Q. B., Morel, J. C., Venkatarama Reddy, B. V., & Ghayad, W. (2009). Durability of rammed earth walls exposed for 20 years to natural weathering. *Building and Environment*. https://doi.org/10.1016/j.buildenv.2008.07.001

Bui, Quoc Bao, Morel, J. C., Hans, S., & Walker, P. (2014). Effect of moisture content on the mechanical characteristics of rammed earth. *Construction and Building Materials*, *54*, 163–169. https://doi.org/10.1016/j.conbuildmat.2013.12.067

Chen, Y., Xia, C., Shepard, Z., Smith, N., Rice, N., Peterson, A. M., & Sakulich, A. (2017). *Self-Healing Coatings for Steel-Reinforced Concrete*. https://doi.org/10.1021/acssuschemeng.6b03142

Ciancio, D., & Gibbings, J. (2012). Experimental investigation on the compressive strength of cored and molded cement-stabilized rammed earth samples. *Construction and Building Materials*, *28*(1), 294–304. https://doi.org/10.1016/j.conbuildmat.2011.08.070

Ciancio, D., Jaquin, P., & Walker, P. (2013). Advances on the assessment of soil suitability for rammed earth. *Construction and Building Materials*, *42*, 40–47. https://doi.org/10.1016/j.conbuildmat.2012.12.049

Easton, D. (2007). *The rammed earth house*. Chelsea Green Publishing.

Eires, R., Camões, A., & Jalali, S. (2017). Enhancing water resistance of earthen buildings with quicklime and oil. *Journal of Cleaner Production*, *142*, 3281–3292. https://doi.org/10.1016/j.jclepro.2016.10.141

Fang, S., Zhang, H., Zhang, B., & Li, G. (2014). International Journal of Adhesion & Adhesives A study of Tung-oil – lime putty — A traditional lime based mortar. *International Journal of Adhesion and Adhesives*, *48*, 224–230. https://doi.org/10.1016/j.ijadhadh.2013.09.034

Gu, K., & Chen, B. (2020). Loess stabilization using cement , waste phosphogypsum , fly ash and quicklime for self-compacting rammed earth construction. *Construction and Building Materials*, *231*, 117195. https://doi.org/10.1016/j.conbuildmat.2019.117195

Hall, M., & Allinson, D. (2009). Assessing the effects of soil grading on the moisture content-dependent thermal conductivity of stabilised rammed earth materials. *Applied Thermal Engineering*, *29*(4), 740–747. https://doi.org/10.1016/j.applthermaleng.2008.03.051

Holub, M., Stone, C., Balintova, M., & Grul, R. (2015). Intrinsic hydrophobicity of rammed earth. *IOP Conference Series: Materials Science and Engineering*, *96*(1). https://doi.org/10.1088/1757-899X/96/1/012024

Jaquin, P. A., Augarde, C. E., Gallipoli, D., & Toll, D. G. (2009). The strength of unstabilised rammed earth materials. *Geotechnique*, *59*(5), 487–490. https://doi.org/10.1680/geot.2007.00129

Lazzari, M., & Chiantore, O. (1999). Drying and oxidative degradation of linseed oil. *Polymer Degradation and Stability* 65, 303–313.

Leelamanie, D. A. L., Karube, J., & Yoshida, A. (2008). Characterizing water repellency indices: Contact angle and water drop penetration time of hydrophobized sand. *Soil Science & Plant Nutrition*, *54*(2), 179–187.

Letey, J., Carrillo, M. L. K., & Pang, X. P. (2000). Approaches to characterize the degree of water repellency. *Journal of Hydrology*, *231*, 61–65.

Li, H., Cui, Y., Li, Z., Zhu, Y., & Wang, H. (2018). Progress in Organic Coatings Fabrication of microcapsules containing dual-functional tung oil and properties suitable for self-healing and self-lubricating coatings. *Progress in Organic Coatings*, *115*(July 2017), 164–171. https://doi.org/10.1016/j.porgcoat.2017.11.019

Lin, H., Lourenço, S. D. N., Yao, T., Zhou, Z., Yeung, A. T., Hallett, P. D., Paton, G. I., Shih, K., Hau, B. C. H., & Cheuk, J. (2019). Imparting water repellency in completely decomposed granite with Tung oil. *Journal of Cleaner Production*, *230*, 1316–1328. https://doi.org/10.1016/j.jclepro.2019.05.032

Lin, Hongjie, & Lourenço, S. D. N. (2020). Physical degradation of hydrophobized sands. *Powder Technology*, *367*, 740–750. https://doi.org/10.1016/j.powtec.2020.04.015

Lin, Hongjie, Zheng, S., Lourenço, S. D. N., & Jaquin, P. (2017). Characterization of coarse soils derived from igneous rocks for rammed earth. *Engineering Geology*, *228*(August), 137–145. https://doi.org/10.1016/j.enggeo.2017.08.003

Liu, D., Lourenço, S. D. N., & Yang, J. (2019). Critical state of polymer-coated sands. *Geotechnique*, *9*, 841–846.

Lourenço, S. D. N. (2015). Wettability of crushed air-dried minerals. *Géotechnique Letters*, *5*(July–September), 173–177. https://doi.org/10.1680/geolett.15.00075

Lourenço, S. D. N., Saulick, Y., Zheng, S., Kang, H., Liu, D., Lin, H., & Yao, T. (2018). Soil wettability in ground engineering: fundamentals, methods, and applications. *Acta Geotechnica*, *13*(1). https://doi.org/10.1007/s11440-017-0570-0

Lourenço, S. D. N., Woche, S. K., Bachmann, J., & Saulick, Y. (2015). Wettability of crushed air-dried minerals. *Geotechnique Letters*, *5*(3), 173–177. https://doi.org/10.1680/jgele.15.00075

Luo, Y., Yang, M., Ni, P., Peng, X., & Yuan, X. (2020). Degradation of rammed earth under wind-driven rain: The case of Fujian Tulou, China. *Construction and Building Materials*, *261*, 119989. https://doi.org/10.1016/j.conbuildmat.2020.119989

Maskell, D., Heath, A., & Walker, P. (2014). Comparing the environmental impact of stabilisers for unfired earth construction. *Key Engineering Materials*, *600*, 132–143. https://doi.org/10.4028/www.scientific.net/KEM.600.132

Meek, A. H., Beckett, C. T. S., & Elchalakani, M. (2020). Alternative stabilised rammed earth materials incorporating recycled waste and industrial by-products : Durability with and without water repellent. *Construction and Building Materials*, *265*, 120629. https://doi.org/10.1016/j.conbuildmat.2020.120629

Mgbemena, C. O. (2013). Determination of the Contact Angles of Kaolin Intercalates of Oleochemicals Derived from Rubber Seed (HeveaBrasiliensis) and Tea Seed (CameliaSinensis) Oils by the Capillary Rise Method. *International Journal of Materials Science and Applications*, *2*(3), 99. https://doi.org/10.11648/j.ijmsa.20130203.15

Nagaraj, H. B., & Muguda, S. (2020). *Recent Innovations in Stabilized Earthen Construction*. Springer International Publishing. https://doi.org/10.1007/978-3-030-46800-2_7

Nakamatsu, J., Kim, S., Ayarza, J., Ramírez, E., Elgegren, M., & Aguilar, R. (2017). Eco-friendly modification of earthen construction with carrageenan: Water durability and mechanical assessment. *Construction and Building Materials*. https://doi.org/10.1016/j.conbuildmat.2017.02.062

NZS 4298:2020, 2020. Materials and construction for earth buildings. Standards New Zealand, New Zealand.

Qiang, S., Zhang, H., Jian, B., & Zheng, Y. (2014). The identification of organic additives in traditional lime mortar. *Journal of Cultural Heritage*, *15*(2), 144–150. https://doi.org/10.1016/j.culher.2013.04.001

Reddy, B. V. V., & Kumar, P. P. (2011). *Cement stabilised rammed earth . Part B : compressive strength and stress – strain characteristics*. 695–707. https://doi.org/10.1617/s11527-010-9659-8

Reddy, B. V. V., Ph, D., Suresh, V., Rao, K. S. N., & Ph, D. (2008). Characteristic Compressive Strength of Cement-Stabilized Rammed Earth. *Journal of Materials in Civil Engineering*, 1–7. https://doi.org/10.1061/(ASCE)MT.1943-5533

Samadzadeh, M., Boura, S. H., Peikari, M., Ashrafi, A., & Kasiriha, M. (2011). Progress in Organic Coatings Tung oil : An autonomous repairing agent for self-healing epoxy coatings. *Progress in Organic Coatings*, *70*(4), 383–387. https://doi.org/10.1016/j.porgcoat.2010.08.017

Saulick, Y., Lourenço, S. D. N., Baudet, B. A., Woche, S. K., & Bachmann, J. (2018). Physical properties controlling water repellency in synthesized granular solids. *European Journal of Soil Science*, *69*(4), 698–709. https://doi.org/10.1111/ejss.12555

Schönemann, A., & Edwards, H. G. M. (2011). *Raman and FTIR microspectroscopic study of the alteration of Chinese tung oil and related drying oils during ageing*. 1173–1180. https://doi.org/10.1007/s00216-011-4855-0

Siddiqua, S., & Barreto, P. N. M. (2018). Chemical stabilization of rammed earth using calcium carbide residue and fly ash. *Construction and Building Materials*, *169*, 364–371. https://doi.org/10.1016/j.conbuildmat.2018.02.209

Sridharan, A., & Sivapullaiah, P. V. (2005). Mini compaction test apparatus for fine grained soils. *Geotechnical Testing Journal*, *28*(3), 240–246.

Tang, X. W., Ying, F., & Lin, T. S. (2006). Properties of Clay Mixed with Sticky Rice Juice and Tung Oil. In *Advances in Unsaturated Soil, Seepage, and Environmental Geotechnics* (pp. 346–353).

Tang, X., Wang, Y., Lin, T., & Lin, J. (2010). Permeability and durability of soils improved by tung oil and sticky rice juice...[J]. *Chinese Journal of Geotechnical Engineering*, *32*(3), 351–354.

Treloar, G. J., Owen, C., & Fay, R. (2001). Environmental assessment of rammed earth construction systems. *Structural Survey*, *19*(2), 99–106. https://doi.org/10.1108/02630800110393680

Walker, P., Keable, R., Martin, J., Maniatidis, V., 2005. Rammed Earth: Design and

Construction Guideline. Building Research Establishment, Watford.

Wessel, A. T. (1988). On using the effective contact angle and the water drop penetration time for classification of water repellency in dune soils. *Earth Surface Processes and Landforms*, *13*(6), 555–561.

Xin, J., Li, M., Li, R., Wolcott, M. P., & Zhang, J. (2016). *Article A green epoxy resin system based on lignin and tung oil and its application in epoxy asphalt A green epoxy resin system based on lignin and tung oil and its application in epoxy asphalt*. https://doi.org/10.1021/acssuschemeng.6b00256

Yan, K., Peng, Y., & You, L. (2020). Use of tung oil as a rejuvenating agent in aged asphalt: Laboratory evaluations. *Construction and Building Materials*. https://doi.org/10.1016/j.conbuildmat.2019.117783

Yang, X., Zhang, S., & Li, W. (2015). Progress in Organic Coatings The performance of biodegradable tung oil coatings. *Progress in Organic Coatings*, *85*, 216–220. https://doi.org/10.1016/j.porgcoat.2015.04.015

Zhang, H. yuan, Zhu, S. bin, Li, M., & Zhang, X. chao. (2016). Water Repellency of Monument Soil Treated by Tung Oil. *Geotechnical and Geological Engineering*. https://doi.org/10.1007/s10706-015-9939-8

Zhang, Q., Chen, W., & Fan, W. (2020). Protecting earthen sites by soil hydrophobicity under freeze–thaw and dry–wet cycles. *Construction and Building Materials*, *262*. https://doi.org/10.1016/j.conbuildmat.2020.120089

Table 1. Properties of completely decomposed granite

Property & composition		
Moisture content (%)		<3.0
Organic matter (%)		<2.0
Specific gravity		2.68
Atterberg limits (%)	Liquid limit	44
	Plastic limit	28
Particle size distribution	Clay (%)	18
	Silt (%)	17
	Sand (%)	49
	Gravel (%)	16
Mineral composition	Quartz (%)	46
	Kaolinite (%)	43
	Illite (%)	6
	Gibbsite (%)	5

Table 2. Properties of Tung oil (*after* Lin *et al.,* 2019; Zhang *et al.,* 2016)

Property		*Description*
Appearance		Transparent with amber colour
Density		0.94×10^3 kg/m^3
Moisture or impurities (%)		0.5
Chemical composition (%)	Alpha-eleostearic acid	~80
	Linoleic acid,	~20
	Palmitic acid,	
	Oleic acid	

Table 3. Testing parameters of Standard Proctor and modified compaction tests

Parameter	*Standard Proctor test*	*Modified compaction test*
Compaction energy (kJ/m^3)	594	572
Height of drop (m)	0.305	0.245
Rammer weight (kg)	2.5	0.397
Volume of mould (cm^3)	1000	85.06
Number of layers	3	3
Number of blows per layer	25	17

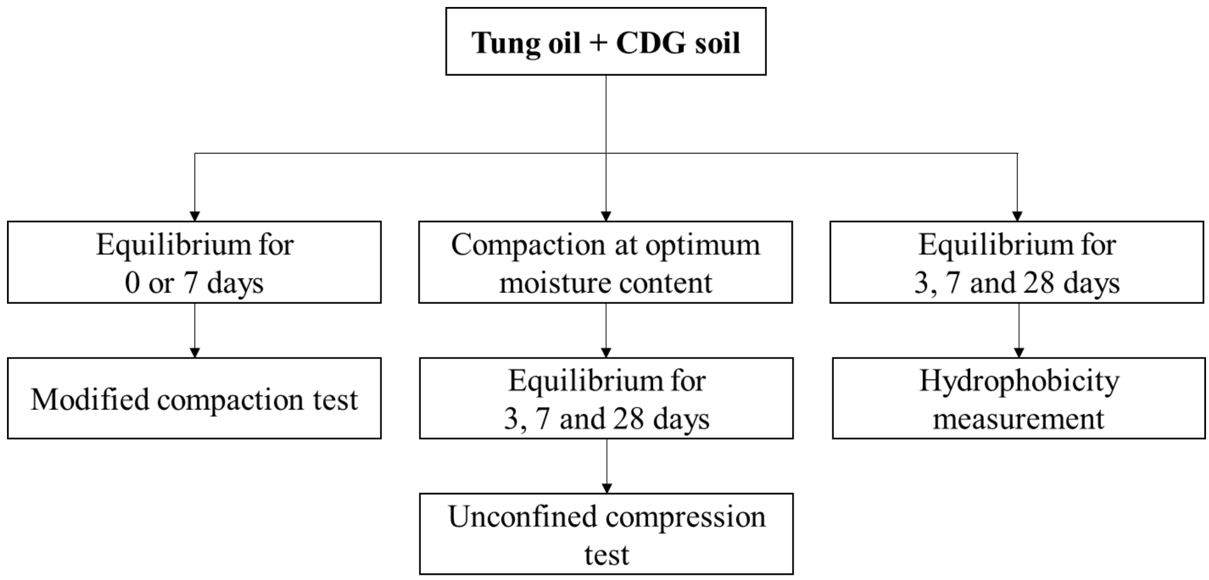

Figure 1. Testing procedure workflow (CDG - completely decomposed granite)

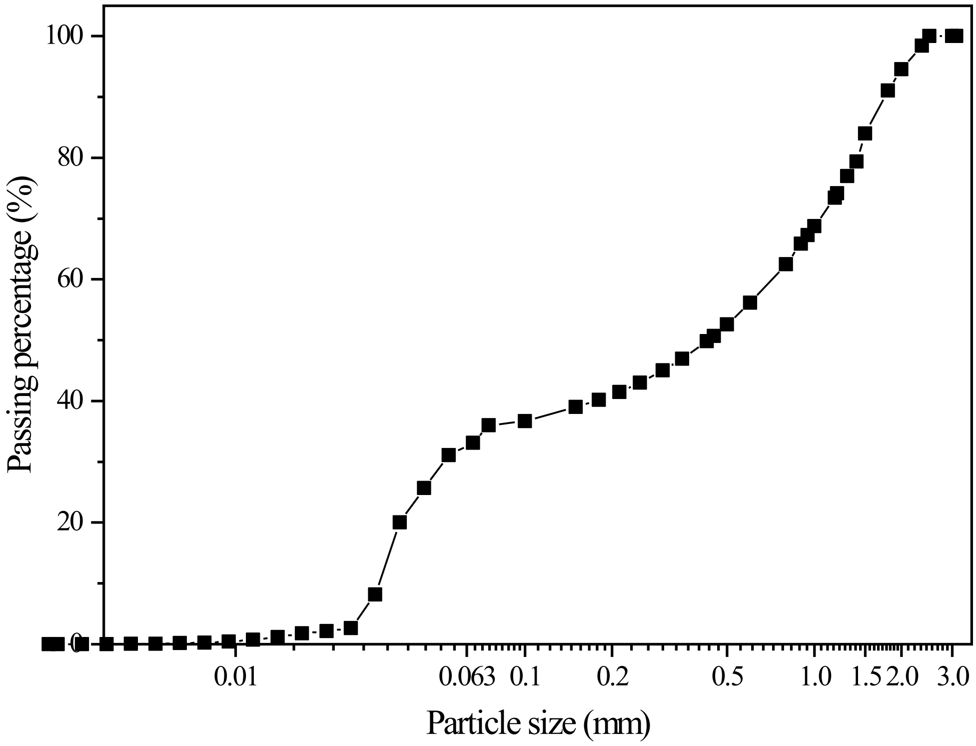

Figure 2. Particle size distribution curve of completely decomposed granite

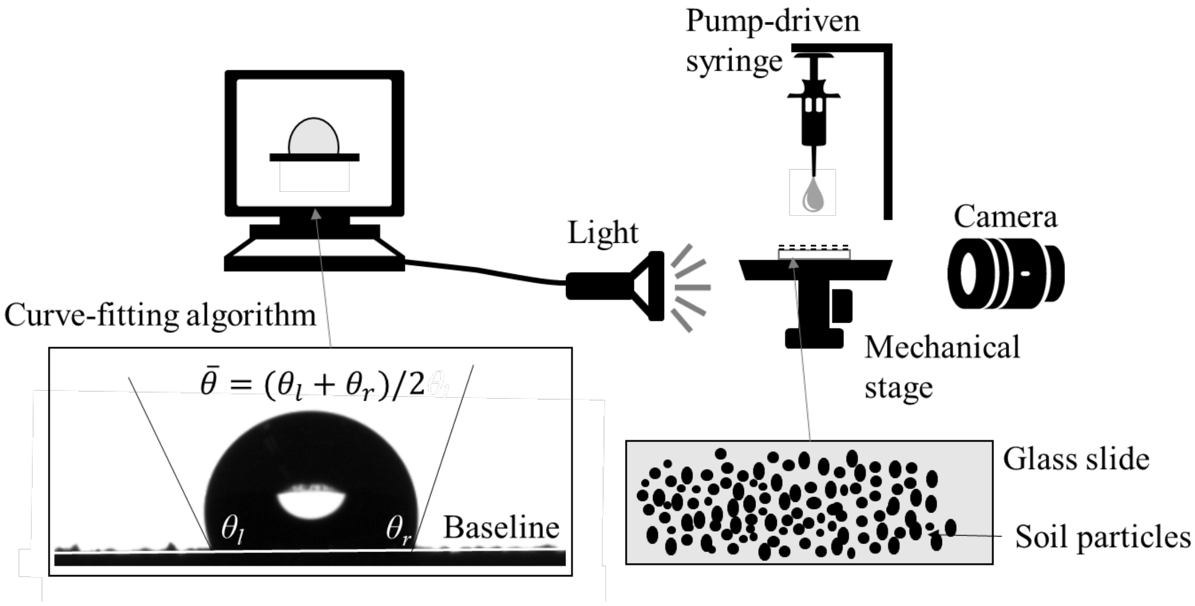

Figure 3. Schematic of sessile drop method for contact angle measurement on soils

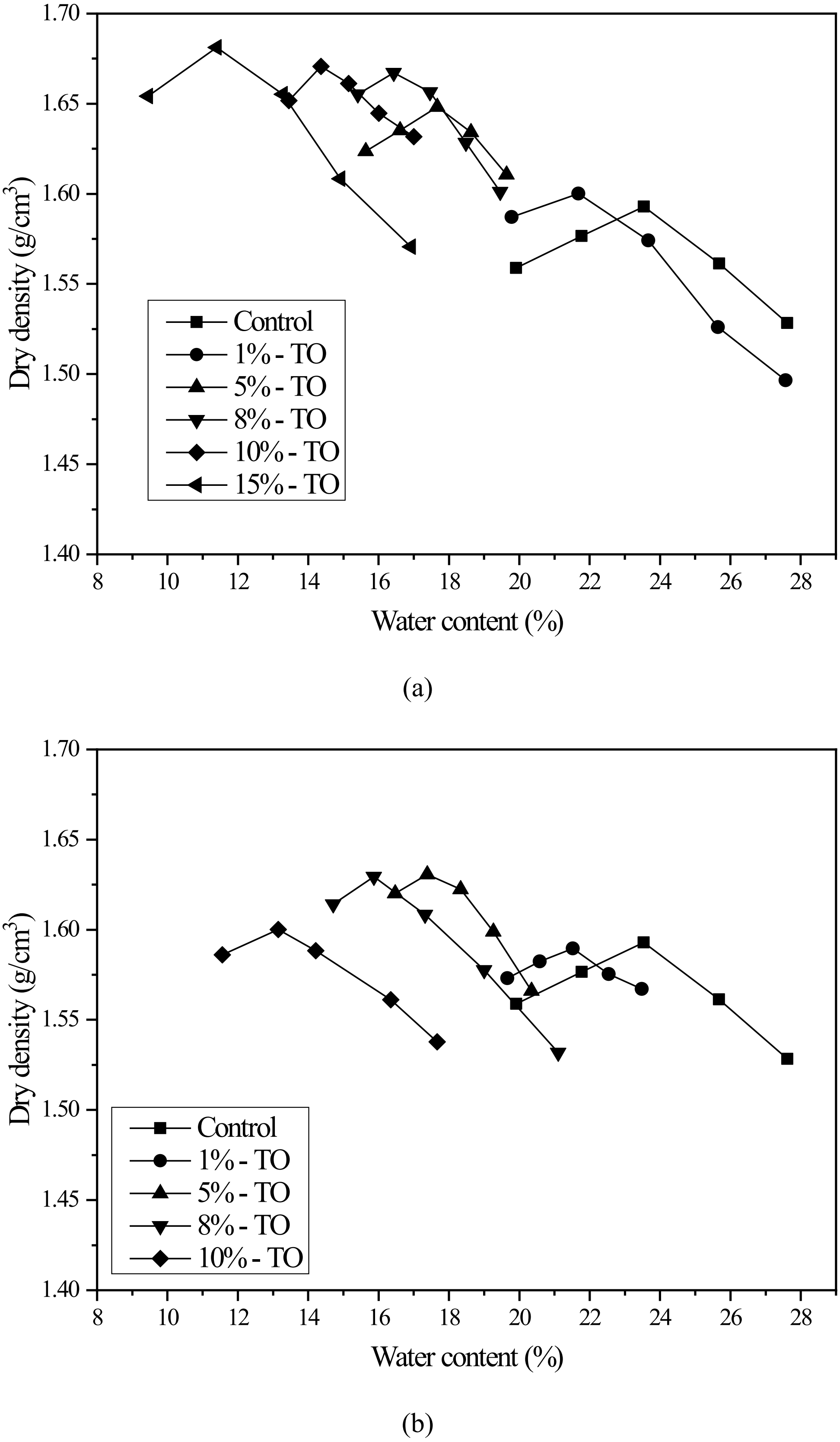

Figure 4. Compaction curves of Tung oil-stabilized completely decomposed granite (a) compaction immediately after mixing and, (b) after 7-day equilibrium

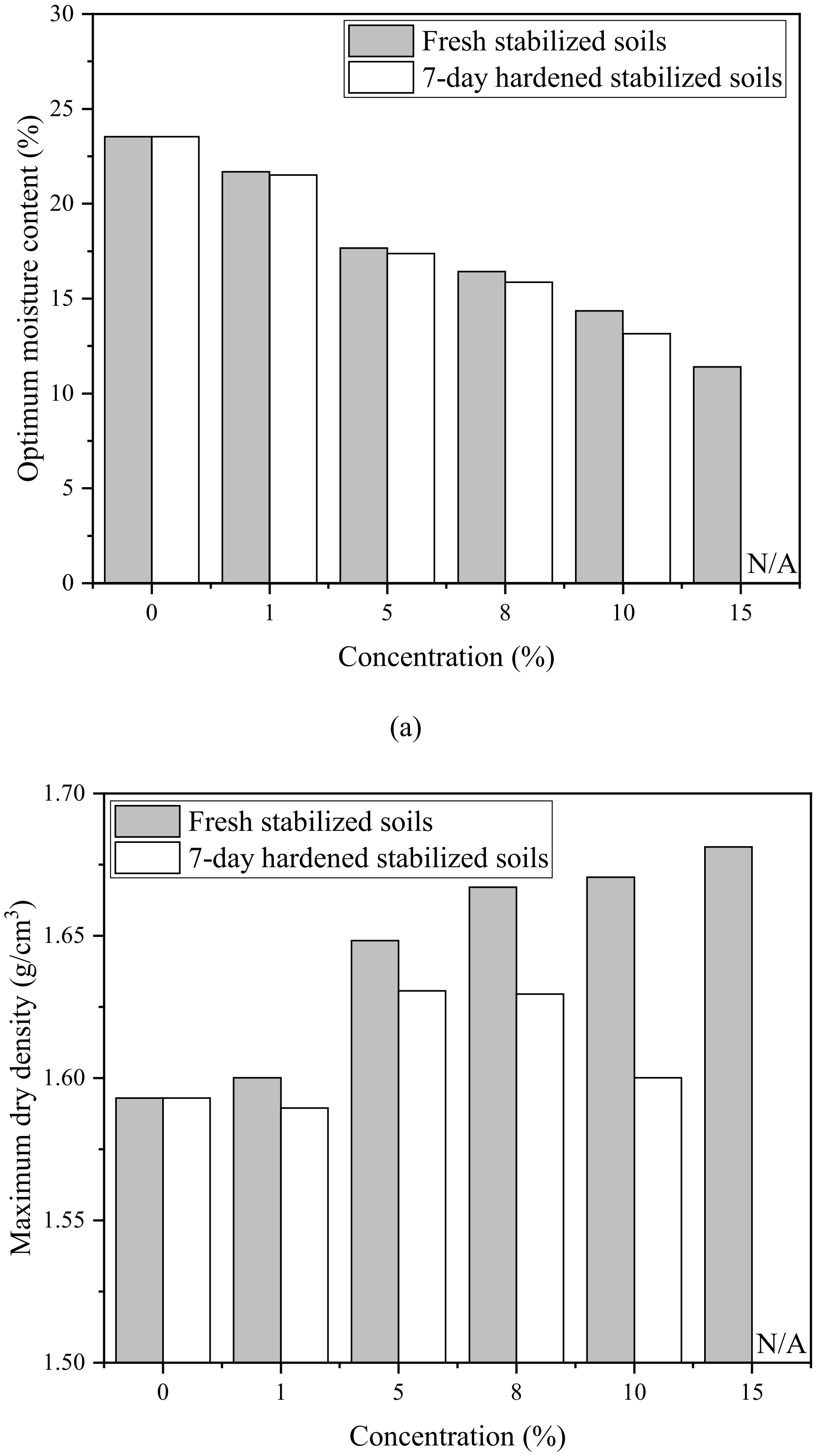

(a)

(b)

Figure 5. Relation between Tung oil concentration and (a) optimum moisture content and, (b) maximum dry density immediately after compaction and after 7-day equilibrium

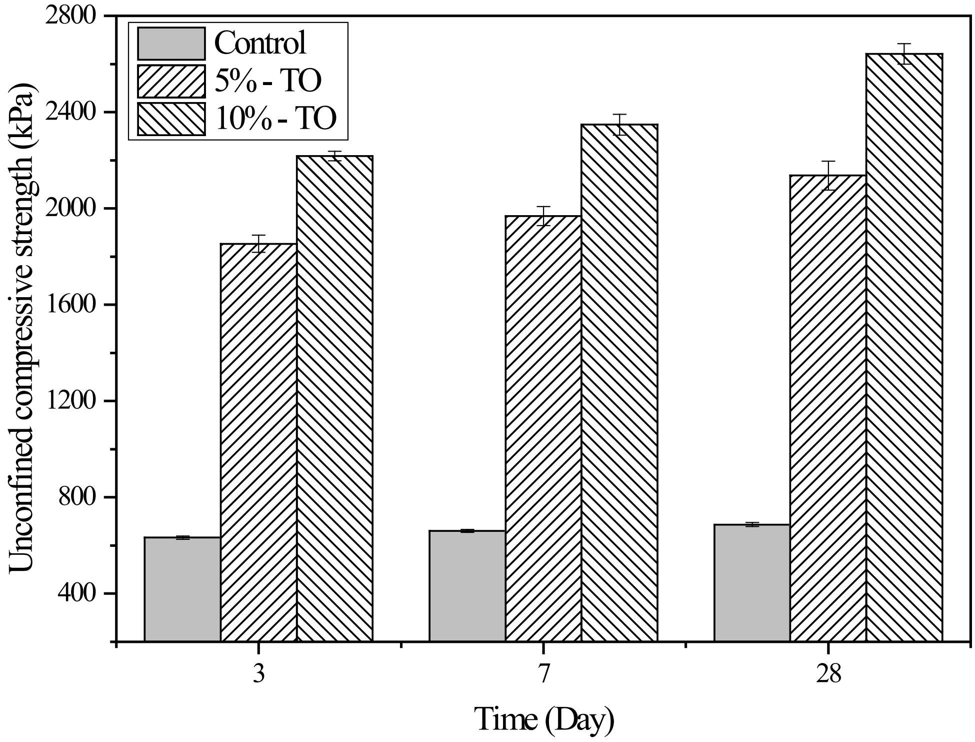

Figure 6. Unconfined compression strength of natural and stabilized completely decomposed granite after 3, 7, 28 days

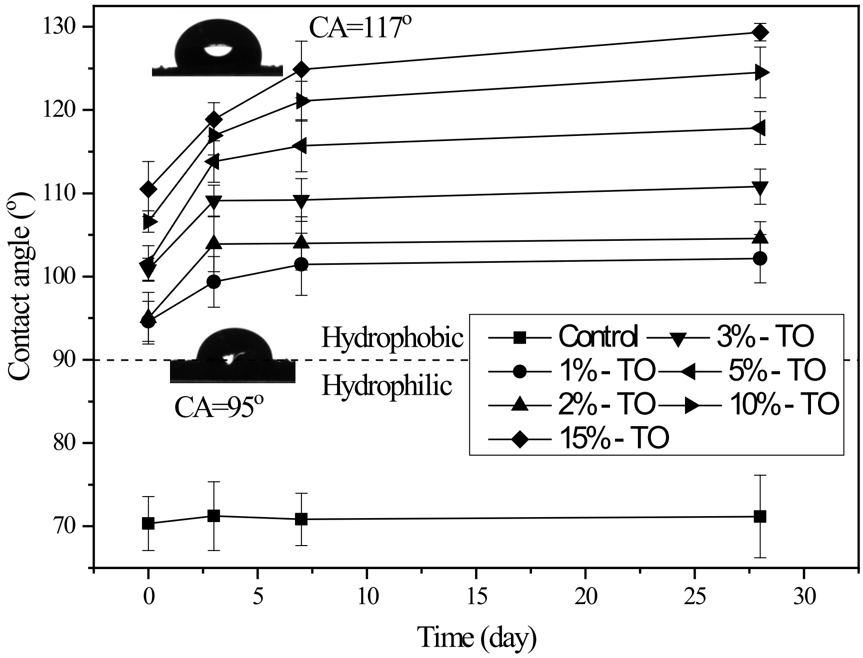

(a)

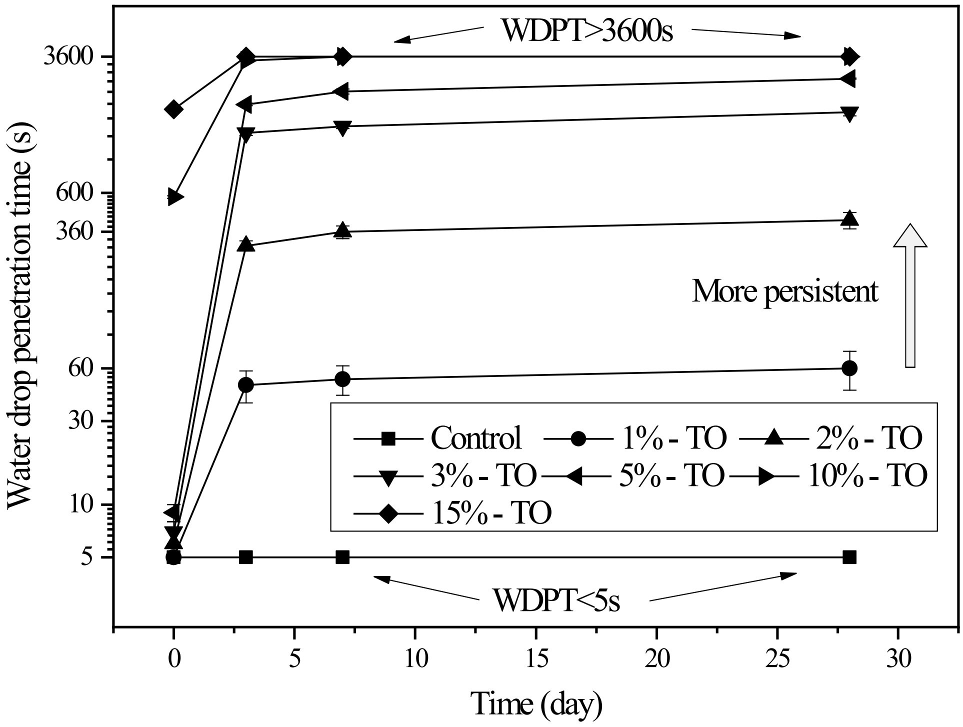

(b)

Figure 7. Completely decomposed granite hydrophobicity induced by Tung oil during 28 days; (a) contact angles and, (b) water drop penetration time

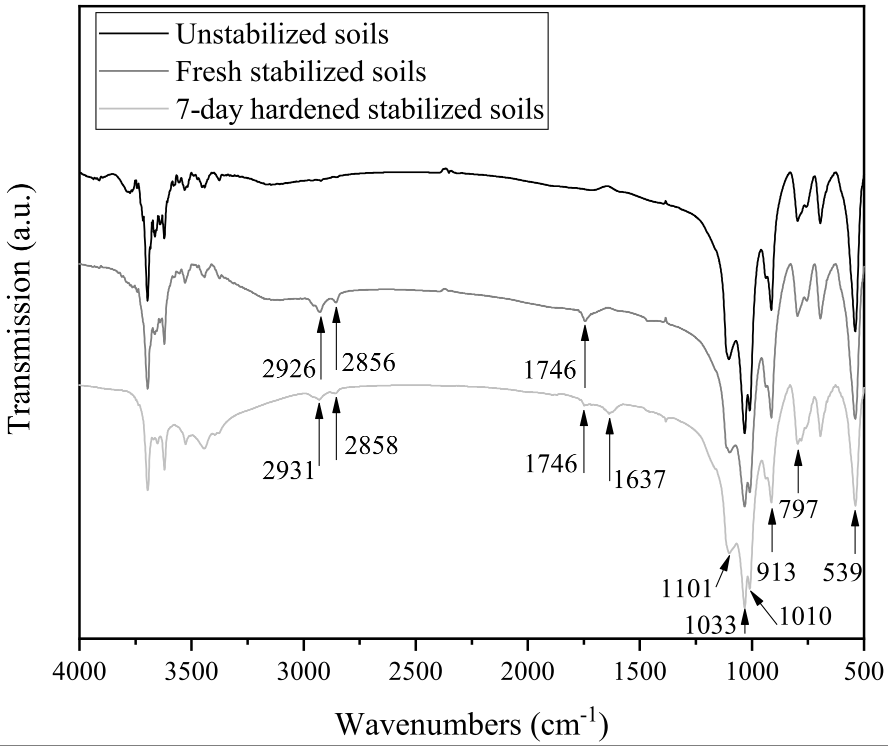

Wavenumber (cm^{-1})		Assignment (moiety and source)
Fresh stabilized soils	7-day hardened stabilized soils	
2926	2931	υ (C-H) of fatty acids in oil
2856	2858	υ (C-H) of fatty acids in oil
1746	1746	υ (C=O) of fatty acids in oil
-	1637	υ (C-O) of carboxylate formed in oil
1462	1456	δ (C-H) of methyl in oil
1100	Overlapped	υ (Si-O) of quartz in soil
1035	Overlapped	υ (Si-O) of quartz in soil
913	Overlapped	δ (O-H) of kaolinite in soil

Figure 8. FTIR spectrum of untreated completely decomposed granite, Tung oil-treated CDG immediately after compaction and after 7-day equilibrium; the table shows the assignment of the absorption bands in the spectrum for the fresh and hardened soils

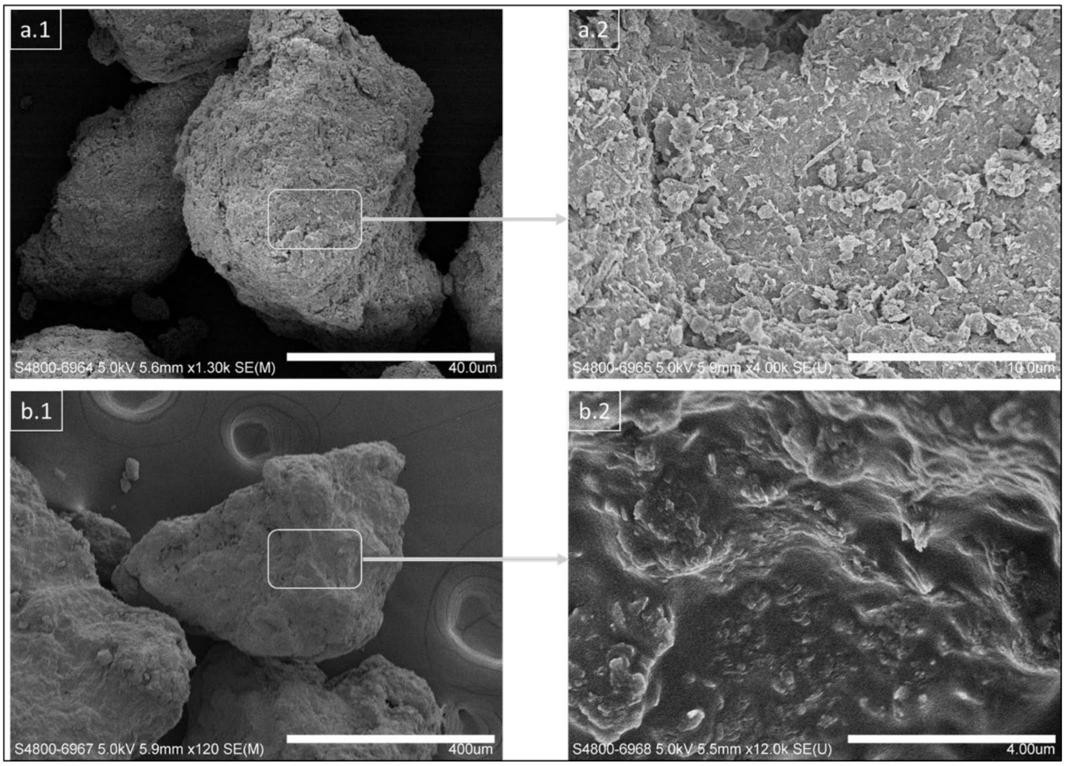

Figure 9. SEM micrographs of (a) natural and (b) stabilized completely decomposed granite with 10% of Tung oil

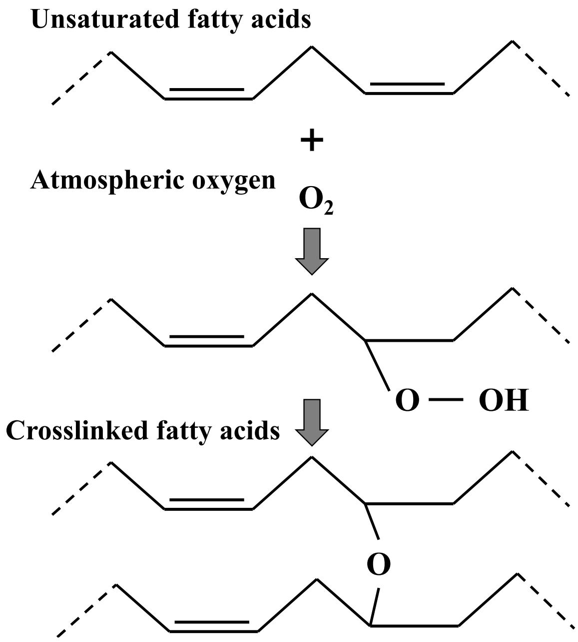

Figure 10. Oxypolymerization of unsaturated fatty acids in Tung oil

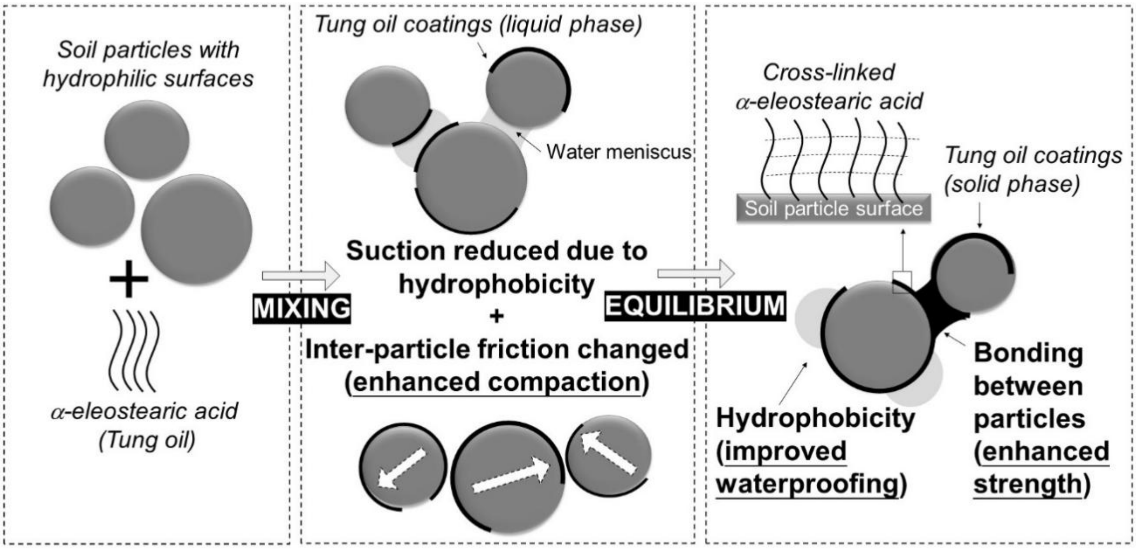

Figure 11. Mechanisms of Tung oil stabilization in an earthen material